Journal of Biomedical Optics

BiomedicalOptics.SPIEDigitalLibrary.org

Nd:YAG laser combined with gold nanorods for potential application in port-wine stains: an *in vivo* study

Linzhuang Xing
Bin Chen
Dong Li
Wenjuan Wu
Guoxiang Wang

SPIE.

Linzhuang Xing, Bin Chen, Dong Li, Wenjuan Wu, Guoxiang Wang, "Nd:YAG laser combined with gold nanorods for potential application in port-wine stains: an *in vivo* study," *J. Biomed. Opt.* **22**(11), 115005 (2017), doi: 10.1117/1.JBO.22.11.115005.

Nd:YAG laser combined with gold nanorods for potential application in port-wine stains: an *in vivo* study

Linzhuang Xing,[a] Bin Chen,[a,*] Dong Li,[a] Wenjuan Wu,[a] and Guoxiang Wang[a,b]
[a]Xi'an Jiaotong University, State Key Laboratory of Multiphase Flow in Power Engineering, Xi'an, Shaanxi, China
[b]University of Akron, Department of Mechanical Engineering, Akron, Ohio, United States

Abstract. Neodymium:yttrium aluminum garnet (Nd:YAG) lasers exhibit considerable potential for treating deeply buried port-wine stains. However, the application of Nd:YAG laser is limited by its weak absorption to blood. This *in vivo* study tested the efficacy and safety of utilizing thiol-terminated methoxypolyethylene glycol-modified gold nanorods (PEG-GNRs) to enhance the absorption of Nd:YAG laser to blood. Mouse mesentery and dorsal skinfold chamber (DSC) model were prepared to analyze the thermal responses of a single venule without anatomic structures, as well as blood vessels in the complex structure of the skin, to laser light. After the injection of 0.44 mg of PEG-GNRs, the required threshold density of laser energy for blood coagulation and complete vasoconstriction decreased from 24 to 18 J/cm^2 in the mesentery model and from 36 to 31 J/cm^2 in the DSC model. The laser pulse required for blood coagulation and complete vasoconstriction decreased by 67.75% and 62.25% on average in the mesentery model and by 67.55% and 54.45% on average in the DSC model. Histological and histochemical results confirmed that PEG-GNRs are nontoxic in the entire mouse life span. Therefore, combining PEG-GNRs with Nd:YAG laser may be effective and safe for inducing an obvious thermal response of blood vessels under low energy density and minimal pulse conditions. [DOI: 10.1117/1.JBO.22.11.115005]

Keywords: port-wine stains; laser dermatology; PEG-modified gold nanorods; mesentery model; dorsal skinfold chamber model.
Paper 170475RR received Jul. 19, 2017; accepted for publication Nov. 6, 2017; published online Nov. 23, 2017.

1 Introduction

Port-wine stains (PWS) are the most common congenital vascular malformations with an incidence of 3 per 1000 newborns.[1] PWS are characterized by ectatic capillaries with diameters varied from 30 to 300 μm and are predominantly located in the papillary and midreticular layers of the dermis.[2,3] The majority of PWS initially appears as flat, pale pink to red patches, and can progressively darken and thicken with age; this change significantly impedes the psychosocial development and well-being of a patient, particularly when lesions occur in exposed regions, such as the head and neck.[4] The selective photothermolysis proposed by Anderson and Parrish[5] has revolutionized PWS treatment. According to this concept, oxy/deoxyhemoglobin within the blood vessels can preferentially absorb and convert laser light into heat inside aberrant blood vessels, thereby resulting in irreversible damage to the vessel wall.[6] A pulsed dye laser (PDL) with a wavelength of 585/595 nm is considered the gold standard treatment modality for PWS. However, the efficacy of this device is limited for a number of reasons including strong absorption by epidermal melanin and inadequate depth of light penetration. As such, the majority of lesions are incompletely removed. A millisecond-pulsed 1064 nm neodymium: yttrium aluminum garnet (Nd:YAG) laser[7] can penetrate deeper compared with a PDL laser and has potential utility for PWS, but there is considerable risk of scarring with current forms of usage. Combining the Nd:YAG laser with the nanoparticles utilized in this paper has the potential to improve the safety of the Nd:YAG laser while still maintaining efficacy.

Nanomaterial has attracted significant interest in various fields. Gold nanorods (GNRs) are widely used for biomedical applications, such as two-photon imaging, x-ray-computed tomography, drug/gene delivery, biosensing, and cancer therapy;[8–11] these functionalities are attributed to the bulk preparation, intrinsic biocompatibility, tunable absorption band, and highly efficient photothermal conversion of GNRs. Monodispersed GNRs, which can be synthesized through the seeded growth method within several hours, are proven stable and biocompatible *in vivo*. The enhancement of absorption into the blood using laser light via gold nanoparticles is achieved through a unique localized surface plasmon resonance (LSPR) phenomenon and a highly efficient photothermal conversion. GNRs exhibit two absorption bands because of the LSPR phenomenon.[12] The weak transverse band is ~520 nm, which changes slightly with the increase in the aspect ratio (length/width) of GNRs. The strong longitudinal band is proportional to the aspect ratio of GNRs, which can be tuned from visible range to near-infrared range (600 to 1200 nm) by varying the dose of silver ion in preparing GNRs.[13] GNRs will strongly absorb laser energy and excite conduction band electrons when irradiated by laser light with specific wavelengths. Laser energy can be released as heat to the surrounding medium when the excited conduction band electrons decay to the ground state. This phenomenon is known as the photothermal effect of GNRs,[14,15] which is the fundamental basis for the potential

*Address all correspondence to: Bin Chen, E-mail: chenbin@mail.xjtu.edu.cn

1083-3668/2017/$25.00 © 2017 SPIE

thermal damage to tissues by GNRs themselves and drug delivery systems using GNRs as a carrier in biomedical applications.

In our previous study,[16] GNRs with an aspect ratio of 5.89 were prepared to investigate the effect of GNRs on light absorption into the blood. A linear correlation between the blood absorbance at 1064 nm and the concentration of GNRs was obtained. Then, a tissue-like phantom containing a glass capillary with blood was prepared to investigate the laser energy density and pulse number required for blood coagulation.[17] The incident laser energy density required for blood coagulation was reduced by 33.3% from 30 to 20 J/cm^2 after the injection of 0.46 mg of GNRs; laser pulse reduced by 42.9% from 14 to 8. These findings indicated that GNRs combined with Nd:YAG laser may be an innovative technology for treating PWS, whereas a series of *in vivo* experiments is still required to further evaluate the efficacy and safety of GNRs for potential use in treating PWS. This study aims to evaluate the potential application of thiol-terminated methoxypolyethylene glycol-modified gold nanorods (PEG-GNRs) as a candidate for improving the efficacy of the laser treatment of PWS by enhancing the absorption of Nd:YAG laser into the blood. This approach can yield low laser energy density and minimum pulse number required for the obvious thermal damage during MLP treatment. In this study, first, we prepared *in vivo* mesentery and dorsal skinfold chamber (DSC) models to compare laser energy density and laser pulse required for the obvious thermal response of blood to Nd:YAG laser with and without GNRs. Then, we investigated the circulation time and biodistribution of GNRs in mice to analyze the metabolism of GNRs. Finally, the histological and histochemical changes of irradiated skin 1 h after laser irradiation and major organs harvested 30 days after injecting GNRs were compared via hematoxylin and eosin (H&E) staining, respectively. This approach was employed to evaluate the safety of Nd:YAG laser combined with GNRs for inducing obvious thermal damage to the blood vessels.

2 Materials and Methods

2.1 *Synthesis of PEG-GNRs*

GNRs were synthesized in an aqueous solution via the well-established seeded growth method as proposed by Ye et al.[18] After obtaining the hexadecyltrimethylammonium bromide-coated gold nanorods (CTAB-GNRs), the thiol-terminated methoxypolyethylene glycol (mPEG$_{5000}$-SH) was used to replace CTAB and avoid aggregation of GNRs to reduce the highly cytotoxic CTAB bilayers used as a cationic detergent in the well-known seeded growth method. PEG-GNRs were prepared according to the protocol developed by Liao and Hafner.[19] The detailed preparation procedure can be found in our previous work.[16] The final products were resuspended in 100 mL of 0.01 M phosphate-buffered saline (PBS; pH 7.4) for future use.

2.2 *Characterization of GNRs*

The optical absorption spectra of GNRs were recorded through a fiber optic spectrometer (DH-2000-BAL, Ocean Optics, Germany). Transmission electron microscopy (TEM) images were captured using a transmission electron microscope (JEOL2100, Japan) operated at an accelerating voltage of 300 kV. The zeta potential of GNRs dispersed in deionized water was determined by the Zetasizer (Nano ZS-90, Malvern Instruments Ltd., United Kingdom) at room temperature. The concentration of PEG-GNRs in aqueous solution was determined via inductively coupled plasma–optical emission spectroscopy (ICP-OES) (ICEP-9000, SHIMADZU Ltd., Japan).

2.3 *In Vivo Animal Models*

In this study, two *in vivo* animal models, namely, mouse mesentery and DSC models, were used to evaluate the efficacy of Nd:YAG laser combined with PEG-GNRs for inducing the thermal responses of two vessel structures. An individual arteriole–venule pair was obtained in the mesentery model. This pair can be used to analyze the thermal response of a single venule to laser light. A lengthwise fold of dorsal skin exists in the DSC model, where subdermal blood vessels and perivascular tissues can be simultaneously irradiated by laser light. We used this model to examine the thermal response of blood vessels in the complex structure of the skin to laser light.

The preparation of the mesentery model is as follows: female Sprague Dawley (SD) mice with body weight of 100 to 120 g from the animal center of the medical school in Xi'an Jiaotong University were deprived of food for 24 h prior to the surgical procedure to reduce intestinal peristalsis. Mice were anesthetized by intraperitoneal injection of chloral hydrate (500 mg/kg body weight). Medial laparotomy was performed on each mouse by making a small (~1 cm) abdominal incision and exteriorizing the mesentery. Excess fat around the mesenteric blood vessels was gently dissected to avoid interference with incident laser light. Excessive desiccation of exposed mesenteric blood vessels was prevented by applying Ringer's solution preheated to 37°C. Anesthesia was continuously maintained via intraperitoneal infusion of chloral hydrate (100 mg/kg/h) during the surgery and *in vivo* experiments. Finally, the mice were euthanized by intraperitoneal administration of chloral hydrate (8 g/kg body weight) when the experiments were completed.

The second animal model is the DSC model, which was first described by Algire in 1943[20] to replace the microvascular circulation system of clinical PWS. The detailed surgical procedure can be found elsewhere in the literature.[21,22] The dorsal skin was shaved, epilated, and lifted to form a skinfold after the mouse was anesthetized by intraperitoneal injection of chloral hydrate (500 mg/kg body weight). One side of the skin with a 1 cm diameter and the subcutis with the panniculus carnosus were carefully removed to expose the targeted subdermal blood vessels in the underlying intact skin. Then, a pair of titanium window frames was attached to each side of the two skinfolds with screws and sutures. Moreover, a thin glass with

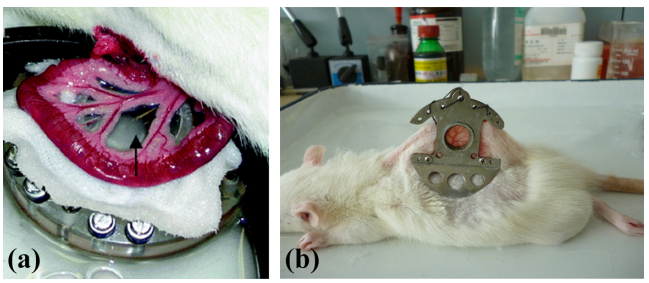

Fig. 1 Two different *in vivo* animal models: (a) mouse mesentery model[23] and (b) mouse dorsal skin chamber model.

the diameter of 12 mm and thickness of 0.2 mm was inserted into the window frame located on the exposed skin surface to prevent exposed subdermal tissues from dehydration and contamination, as shown in Fig. 1. The irradiated skin was harvested at ~1 h after laser irradiation and prepared for a routine histological technique to investigate the effect of PEG-GNRs on perivascular tissues during laser irradiation.

2.4 *Laser Irradiation*

The basic experimental setup was composed of a long-pulsed 1064 nm Nd:YAG laser system (WON-COSJET TR, Won Technology Co., Ltd., Daejeon, Republic of Korea), *in vivo* animal models, a microscopy camera with ×4 magnification (BX41, Olympus Corp., Japan), and a high-speed camera (Model HG-100K, Redlake) with a resolution of 1504 × 1128 pixels and frame rate of 25 to 2000 fps. This setup is shown in Fig. 2.

For *in vivo* experiments, SD mice were assigned to four groups: laser only in mesentery model ($n = 3$); laser combined with PEG-GNRs in mesentery model ($n = 5$); laser only in DSC model ($n = 5$); laser combined with PEG-GNRs in DSC model ($n = 10$). For all laser irradiation experiments, the pulse duration of Nd:YAG laser was 0.3 ms, with a spot diameter of 2 mm and pulse repetition rate of 10 Hz.

All procedures involving animal experiments were approved by the Institutional Animal Care and Use Committees of the Xi'an Jiaotong University.

2.5 *Data Analysis*

The color images of mesentery blood vessels and dorsal skin recorded during the laser irradiation procedure were analyzed to compare the pulse number and the corresponding energy density required for blood photocoagulation and complete vasoconstriction with and without injection of PEG-GNRs, respectively. The dorsal skin exposed to laser light was harvested 1 h after laser irradiation. H&E staining was performed to determine if adverse cutaneous effects occurred. This approach can be used to evaluate the safety of the laser treatment of PWS after adding PEG-GNRs.

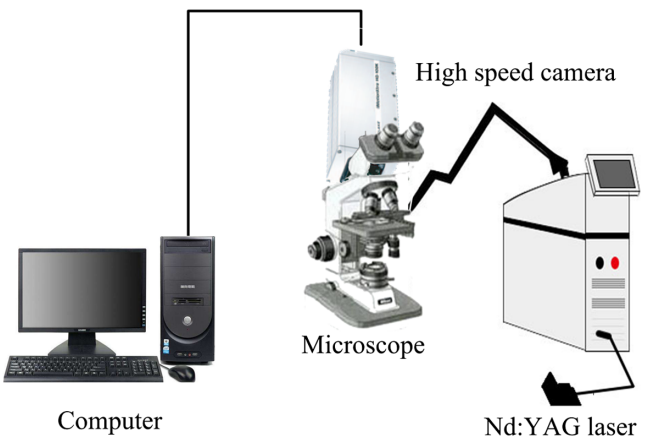

Fig. 2 Schematic of the experimental setup.

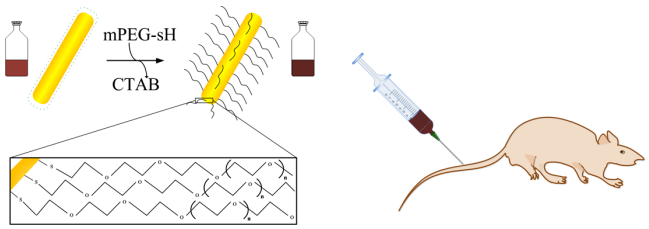

Fig. 3 Schematic of the preparation of PEG-GNRs and the intravenous injection from tail vein.

2.6 *In vivo Circulation Time, Biodistribution, and Histological Analysis of PEG-GNRs*

SD mice were i.v. injected with 0.44 mg of PEG-GNRs dissolved in 200 μL of PBS through the tail vein. This approach was employed to investigate blood circulation behavior, as shown in Fig. 3. Then, 10 μL of blood from the suborbital space was withdrawn at 0, 30 min, 1, 2, 4, 8, 12, 24, 48, and 72 h diluted with 2 mL of PBS containing 0.545-mM sodium citrate. The absorption spectra of blood samples were recorded with a spectrometer to assess the plasmon peak height of PEG-GNRs.

For the biodistribution experiments, the mice were euthanized by intraperitoneal injection of chloral hydrate (8 g/kg body weight) after vascular clearance of PEG-GNRs at 72 h after the injection of PEG-GNRs (0.44 mg). Major organs or tissues, such as liver, kidney, stomach, spleen, lung, heart, skin, and muscle, were collected, wet-weighted, and stored at −20°C for 2 days. Afterward, the organs were triturated, digested in 5 mL digesting solution (HCl/HNO_3 of 3 : 1 by volume), and heated at 90°C for 6 h. After subsequent heating at 140°C for 2 h, the organic compounds were completely oxidized and the gold in the organs was ionized. Finally, the quantitative analysis of Au in various organs was performed by ICP-OES.

Two mice were i.v. injected with 200 μL of PBS and 200 μL of PBS that contains 0.44 mg of PEG-GNRs through the tail vein to perform histological analysis by H&E staining. One mouse without injection was considered the control. Three mice were housed in the same cage and fed a standard diet (three meals per day) for 30 days. The mice were euthanized by intraperitoneal injection of chloral hydrate (8 g/kg body weight). The major organs of each mouse were harvested, rapidly fixed in 4% neutral formalin for 24 h, processed routinely into paraffin, sectioned into thin slices, and stained with H&E for histological analysis.[24]

2.7 *Cell Viability Assay*

The cytotoxicity of PEG-GNRs was assessed using 1.25×10^4 Michigan Cancer Foundation-7 (MCF-7) cells plated in 96-well microplates (Costar, Corning, New York). Then, 0.25 mL of culture medium was added. After incubation for 12 h, coculture wells were exposed to a gradient of PEG-GNRs (0 to 800 μg Au/mL) and incubated for 24 h. Culture medium was then removed and 0.25 mL of fresh culture medium was added together with 100 μL of 5 mg/mL 3-(4,5-dimethylthiazol-2-yl)-2,5-diphenyltetrazolium bromide (MTT). After subsequent incubation for 4 h, culture medium was removed and 1 mL of methyl sulfoxide was added. The absorbance at 570 nm was recorded using a spectrophotometer (SpectraMax, Molecular Devices) to assess the colorimetric viability assay. Triplicates were prepared for the experiments.

3 Results and Discussion

3.1 *Characteristics of PEG-GNRs*

CTAB-GNRs with an aspect ratio of 5.89 were prepared through the seeded growth method. Negatively charged PEG was modified onto the surface of NRs to replace positively charged CTAB. This approach aims to reduce cytotoxicity and avoid aggregation of GNRs. The characteristics of PEG-GNRs are shown in Fig. 4. As shown in Fig. 4(a), the original CTAB-GNRs exhibited two absorption bands, i.e., a weak transverse absorption band at 514 nm and a strong longitudinal absorption band at 1053 nm, which was close to that of the incident Nd:YAG laser. A slight blueshift of the longitudinal absorption band was observed after PEG modification. The longitudinal absorption band of GNRs was dependent on the aspect ratio of GNRs. The shift of the absorption peak of GNRs was due to the local refractive index around the GNRs, which was sensitive to the changes of the GNR surface. In this study, the blueshift of the longitudinal absorption band was due to the binding of PEG onto the surface of GNRs forming the PEG-GNR layer instead of the CTAB-GNR layer. Similar results were reported, which showed that the longitudinal absorption band shift of GNRs can be induced by binding various kinds of biological molecules.[25] No obvious broadening in the longitudinal absorption band was observed during PEGylation, which indicated that aggregates did not exist during PEG-GNR preparation. The TEM images of PEG-GNRs in Fig. 4(b) indicate that the morphology of GNRs was nearly unchanged and good dispersion of the products was achieved. The zeta potentials shown in Fig. 4(c) provided additional evidence of the successful displacement of CTAB by PEG. After modification, the zeta potential of the GNRs reversed from positive (+48.3 mV) to negative (−3.84 mV), which indicated the successful binding of PEG onto the final GNRs. The PEG-GNRs dispersed in deionized water were heated from 30 to 80°C at an interval of 10°C. This approach was conducted using the temperature control system to examine the thermostability of PEG-GNRs. The near-infrared absorption spectra of PEG-GNRs at different temperatures were recorded, as shown in Fig. 4(d). The longitudinal absorption band of PEG-GNRs dispersed in deionized water had a slight blueshift from 1053 to 1040 nm with temperature changing from room temperature to 80°C. This result indicates that the morphology of PEG-GNRs was nearly stable at different temperatures and the PEG-GNRs retained its good thermostability. As reported previously, the blueshift resulted from the decrease in the aspect ratios of GNRs because of the increase in temperature.[26]

3.2 *Thermal Response of Mesentery Blood Vessels After Nd:YAG Laser Irradiation Associated with PEG-GNRs*

In this section, the mesentery vessels of mice were used to analyze the effect of PEG-GNRs on the thermal response of blood vessels to Nd:YAG laser. One example of the evolution of one arteriole–venule pair after exposure to Nd:YAG laser with different laser parameters with and without PEG-GNRs is shown in Fig. 5. Before injection PEG-GNRs, a slight dilation of the venule from initial 300 (±1) to 317 (±3) μm occurred after exposure to the first laser pulse with laser energy density of 36 J/cm^2 (data were not shown). Then, the vessel diameter of the venule increased rapidly from 317 (±3) to 415 (±8) μm after exposure to the second laser pulse because of thermal dilation.

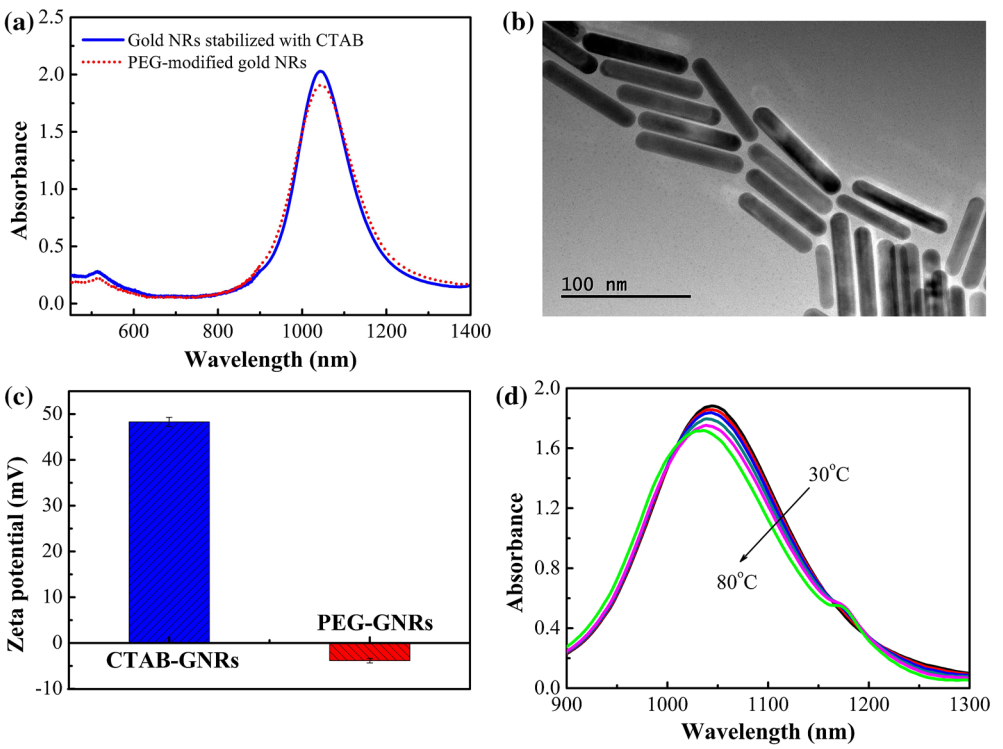

Fig. 4 Characteristics of the prepared PEG-GNRs. (a) Absorption spectra. (b) TEM image of PEG-GNRs. (c) Zeta potential of original CTAB-GNRs and PEG-GNRs. (d) Near-infrared absorption spectra of PEG-GNRs at different temperatures.

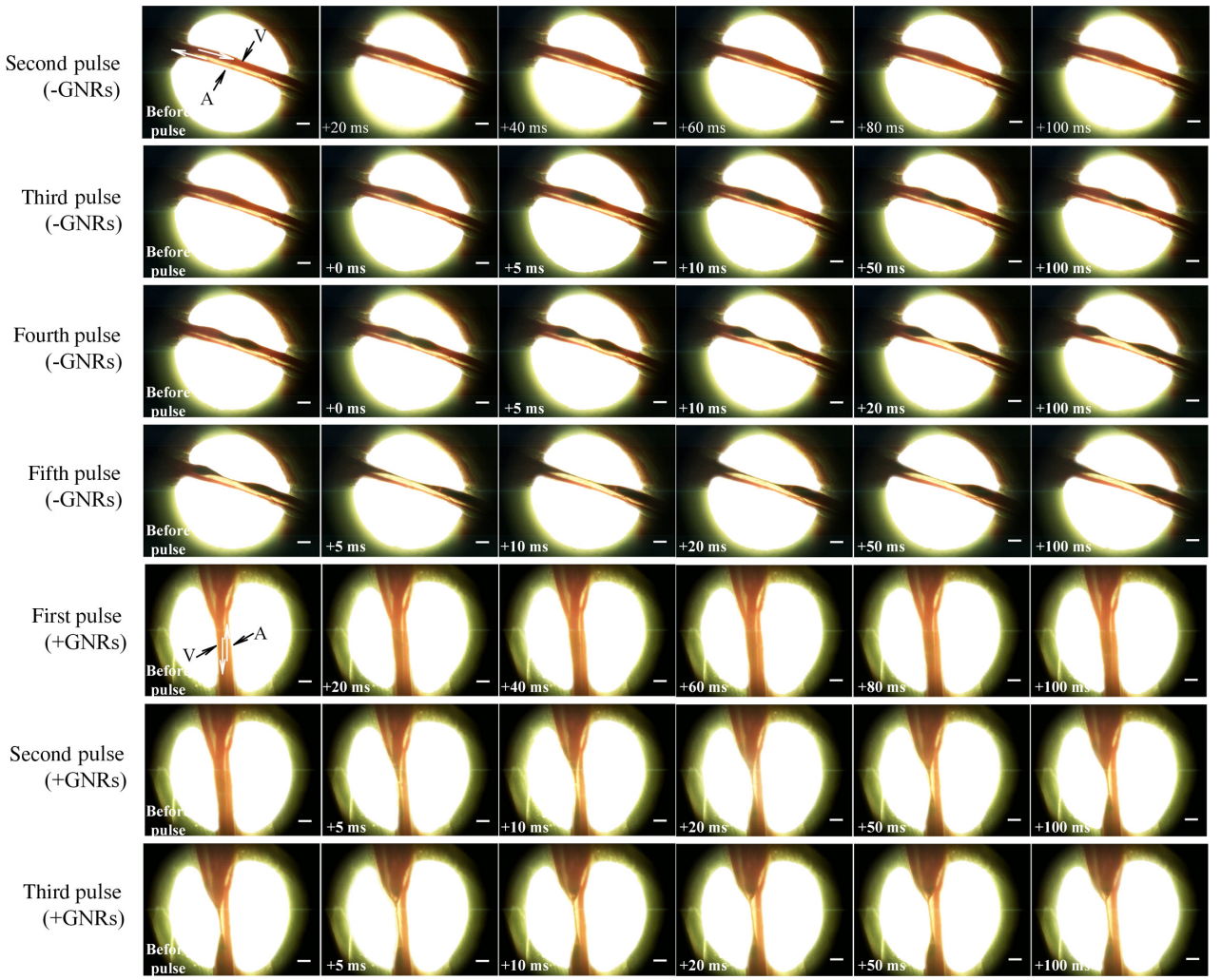

Fig. 5 Video frames of venules and arterioles alongside before and after exposed to different laser pulses. V = venule; A = arteriole; white arrows indicated the direction of blood flow; the time relative to different laser pulses is indicated in the upper left corner; and the scale bars in all pictures are 500 μm. −GNRs means blood vessels without injection of PEG-GNRs were irradiated by laser energy density of 36 J/cm^2, +GNRs means blood vessels with injection of 0.44 mg of PEG-GNRs were irradiated by a laser at an energy density of 24 J/cm^2.

Photocoagulation occurred immediately, which appeared dark when the third laser pulse irradiated the vessel blood. Initial vasoconstriction was observed at 10 ms after laser irradiation, and the vessel diameter of the venule was 249 ($\pm$7) μm at 100 ms after this laser pulse. After exposure to the fourth laser pulse, considerable coagulation formed immediately after laser irradiation. Complete vasoconstriction with the vessel diameter of 33 ($\pm$2) μm was observed at 20 ms. The length of complete vasoconstriction increased over time. Nontransient bubble formation was observed immediately after the fifth laser pulse, and the length of complete vasoconstriction changed slightly. After injection 0.44 mg of PEG-GNRs, the diameter of the blood vessel increased slightly by a factor of 1.11 from an initial diameter of 280 ($\pm$9) to 310 ($\pm$6) μm at 100 ms after the first laser pulse with laser energy density of 24 J/cm^2. Then, coagulation, complete vasoconstriction, and bubble formation were observed immediately after the second laser pulse simultaneously. The length of complete vasoconstriction increased with respect to the time points after this laser pulse, and the bubble disappeared in the direction of blood flow before the next laser pulse. The length of complete vasoconstriction further increased after exposure to the third laser pulse.

These results showed that the laser energy density required to obtain a similar thermal response of venule decreased from 36 to 24 J/cm^2, and the corresponding number of laser pulses decreased from 5 to 3 after injecting 0.44 mg of PEG-GNRs. Therefore, we may conclude that injecting PEG-GNRs into the blood can effectively reduce the laser energy density and laser pulse required for obvious thermal damage. More experiments were conducted to obtain the statistical results. Blood coagulation and complete vasoconstriction were associated with good lesion clearance.[27] Therefore, we statistically investigated the laser energy density and laser pulse required for blood coagulation and complete vasoconstriction with and without PEG-GNRs. A total of eight animals were used in this study group. Eighteen venules without PEG-GNRs and 30 venules with PEG-GNRs were irradiated by Nd:YAG laser with laser energy density changing from 18 to 36 J/cm^2. The detailed results are summarized in Fig. 6. Pertinent results in Fig 6(a) were (i) for laser energy density lower than 24 J/cm^2, blood

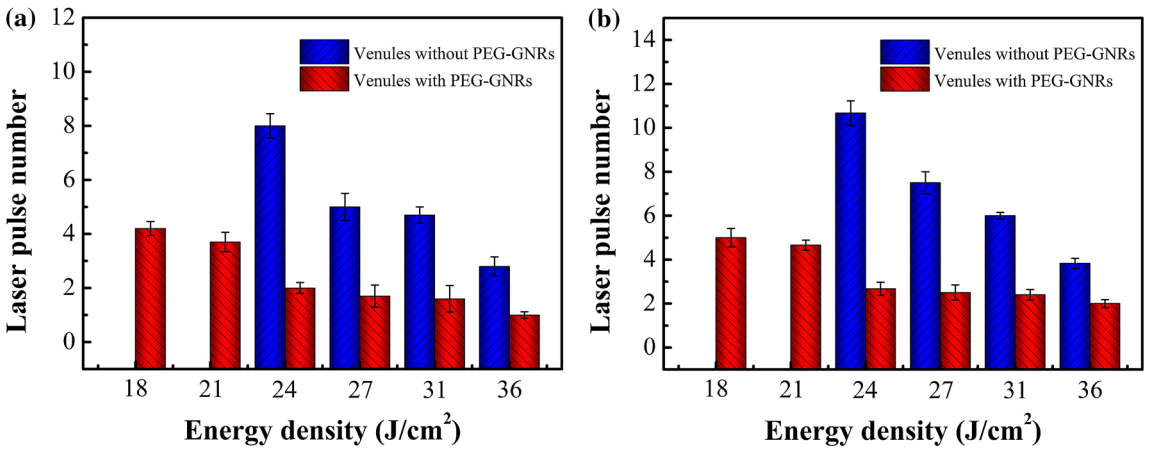

Fig. 6 (a) Laser energy density and pulse number required for coagulation and (b) complete vasoconstriction of venules in mesentery model before and after injection of 0.44 mg of PEG-GNRs.

coagulation can be observed with a total of laser pulses lower than 10 after injecting PEG-GNRs while laser irradiation cannot induce blood coagulation, even if the blood vessel was irradiated for more than 20 laser pulses without PEG-GNRs; and (ii) for each laser energy density, the total number of laser pulses required for blood coagulation with PEG-GNRs was significantly lower than that without PEG-GNRs. When laser energy density was 24, 27, 31, and 36 J/cm^2, the laser pulse required for coagulation decreased by 75%, 66%, 66%, and 64%, respectively. Similar statistical results can be obtained for complete vasoconstriction with or without PEG-GNRs, as shown in Fig. 6(b). When laser energy density was 24, 27, 31, and 36 J/cm^2, the laser pulse required for complete vasoconstriction decreased by 75%, 66%, 60%, and 48%, respectively, after injecting PEG-GNRs.

3.3 *Thermal Response of Dorsal Skin Blood Vessels After Nd:YAG Laser Irradiation Combined with PEG-GNRs*

Figure 7 shows the thermal response of blood vessels with and without injection of PEG-GNRs after exposure to Nd:YAG laser light. Before adding PEG-GNRs, blood coagulation occurred immediately after the sixth pulse. Then, complete vasoconstriction was observed immediately after the ninth pulse. However, blood coagulation was observed after exposure to the third pulse with the injection of 0.44 mg of PEG-GNRs, which decreased by 50%. Complete vasoconstriction was observed after exposure to the sixth laser pulse, which decreased by 33%.

More experiments were conducted to obtain the statistical results. A total of 15 animals were used in this study group. Twelve venules without PEG-GNRs and 24 venules with PEG-GNRs were irradiated by Nd:YAG laser with laser energy density changing from 24 to 36 J/cm^2. The detailed results are summarized in Fig. 8. After adding 0.44 mg of PEG-GNRs, the number of laser pulses required for blood coagulation decreased by 62.5%, 66.7%, 66.7%, and 74.3% when the laser energy was 24, 27, 31, and 36 J/cm^2, respectively. Similarly, the total number of laser pulses required for complete vasoconstriction decreased by 52.5%, 53.3%, 50.5%, and 61.5% when the laser energy was 24, 27, 31, and 36 J/cm^2, respectively. Thus, injecting PEG-GNRs into the blood vessels can effectively reduce the number of laser pulses and the corresponding

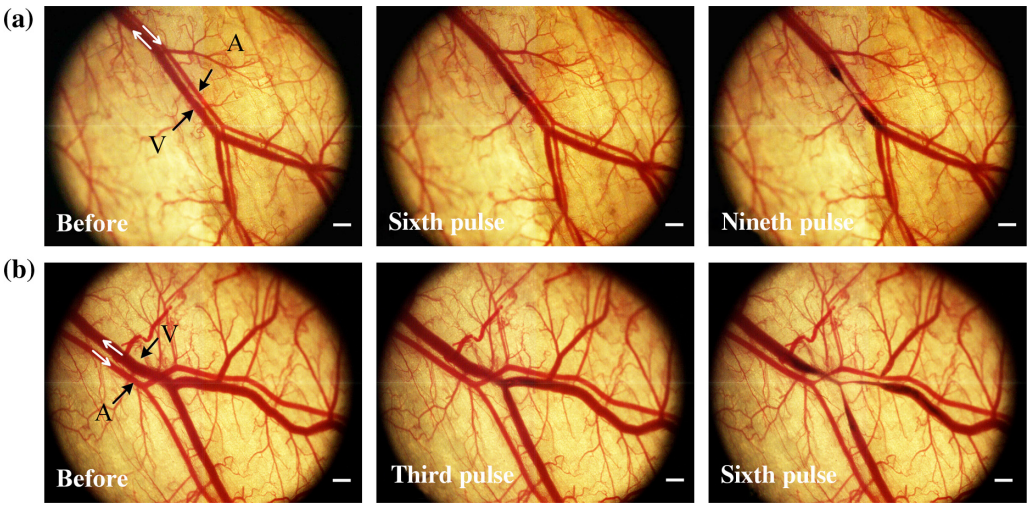

Fig. 7 (a) Thermal response of blood vessels before and after irradiation at laser energy density of 36 J/cm^2 without PEG-GNRs and (b) laser energy density of 31 J/cm^2 with injection 0.44 mg of PEG-GNRs.

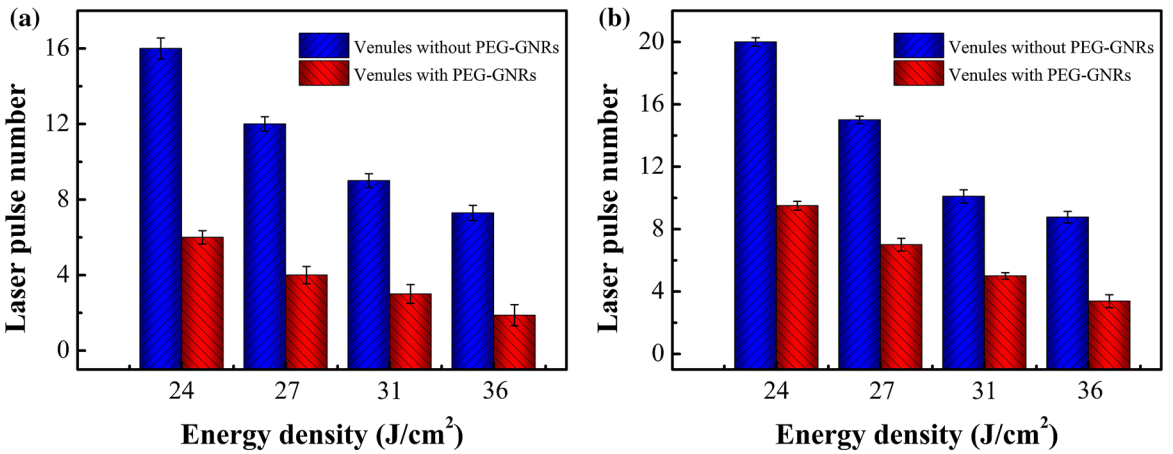

Fig. 8 (a) Laser energy density and pulse number required for coagulation and (b) complete vasoconstriction of venules in DSC model before and after injection of 0.44 mg of PEG-GNRs.

energy density required for blood coagulation and complete vasoconstriction.

3.4 *Biosafety of PEG-GNRs in the Laser Treatment of PWS*

The biosafety of PEG-GNRs on organisms is the most important factor that we must consider cautiously. This study explores the effect of PEG-GNRs on mouse life and perivascular tissues after laser irradiation. In Fig. 9(a), PEG-GNRs exhibited a relatively long half-life of ~3 h in blood circulation because of the essential ultrasmall size of GNRs. The layer of PEG molecules existed between GNRs and the surrounding environment, which could effectively reduce the phagocytosis of macrophages and the adsorption of proteins.[28] Extensive blood circulation time indicated that PEG-GNRs could continuously circulate the blood to the site of the targeted blood vessels and extensively enhance absorption into the blood. The results of biodistribution in Fig. 9(b) indicated that PEG-GNRs were mainly detected in the reticuloendothelial organs, such as the liver, spleen, and lung. High distribution in the spleen with the %ID/g value of ~21% indicated that PEG-GNRs could be excreted via the reticuloendothelial system uptake with splenic clearance dominating hepatic clearance. Similar results were reported, which indicated that the injected PEG-GNRs could be cleared through renal, splenic, and hepatic clearance.[24,29]

The injected mice were fed and observed for 30 days to further assess the long-term effect of PEG-GNRs on the mice life span. The results showed no signs of NR toxicity, such as weakness, labored breathing, or failure to thrive. This finding indicates that the injected dosage of PEG-GNRs was safe for the mice. Major organs, such as the liver, kidney, spleen, lung, and heart, were harvested 30 days after i.v. injecting PEG-GNRs and staining with H&E. As shown in Fig. 10, the H&E images of the major organs were similar to the corresponding major organs of a healthy mouse. This finding further confirms that side effects or toxicity of PEG-GNRs was not observed in mice. The cytotoxicity of PEG-GNRs can be further assessed through cell viability assay, as shown in Fig. 11. The results showed that the cytotoxicity of PEG-GNRs was dependent on the concentration of PEG-GNRs. MCF-7 maintained a high viability of >80% when the concentration of PEG-GNRs was lower than

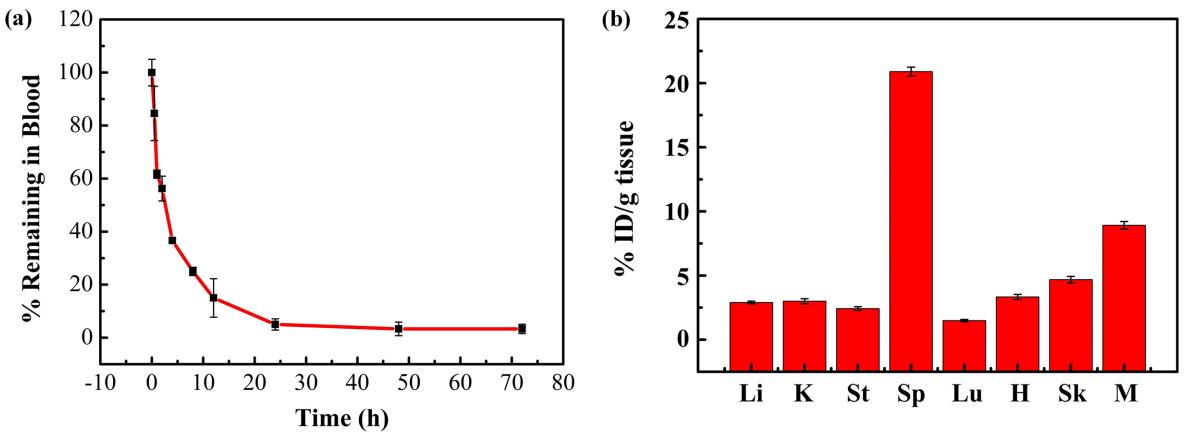

Fig. 9 Circulation time and biodistribution of PEG-GNRs in mice. (a) PEG-GNRs were i.v. administered (4.4 mg/kg) to three mice, and blood was collected over time to monitor the blood clearance of PEG-GNRs from circulation. (b) The biodistribution of PEG-GNRs at 72 h after i.v. administration, as quantified by measuring gold concentrations in tissue lysates via ICP-OES (three mice). Li, liver; K, kidney; St, stomach; SP, spleen; Lu, lung; H, heart; Sk, skin; and M, muscle. %ID/g tissue means the percent of injected dose of PEG-GNRs per gram tissue.

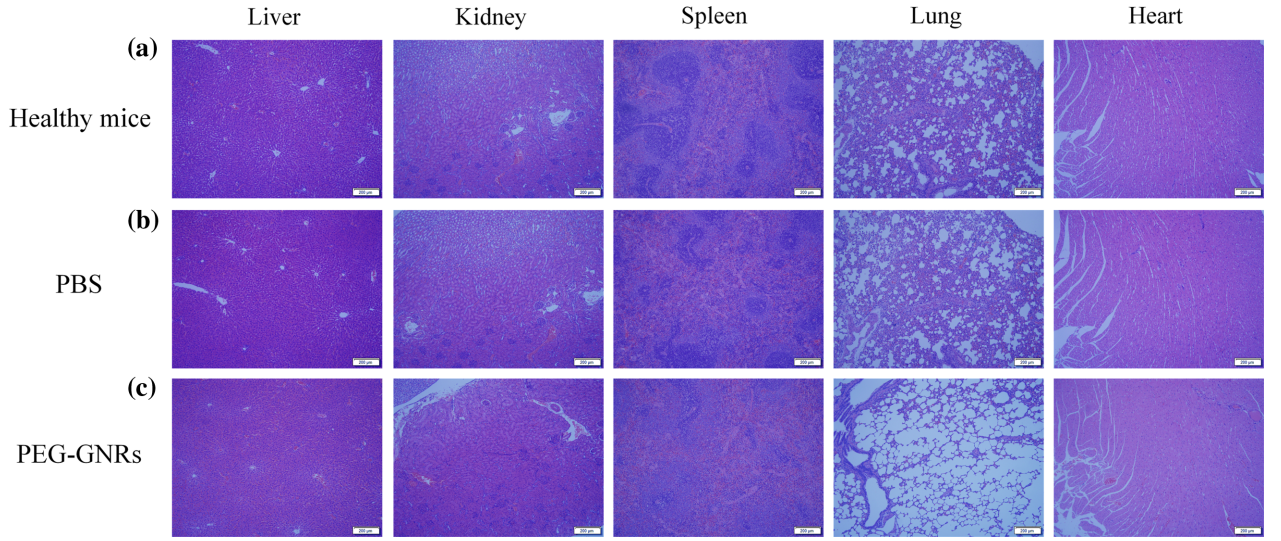

Fig. 10 H&E-stained images of major organs collected from (a) healthy mice, (b) mice i.v. injected with PBS, and (c) mice i.v. injected with PEG-GNRs. The scale bars in all images are 200 μm.

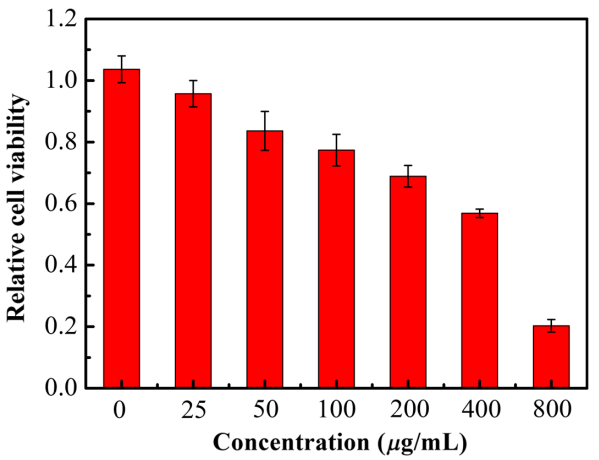

Fig. 11 Quantitation of cellular viability via absorbance of MTT reagent.

100 μg/mL. In our study, the concentration of PEG-GNRs in blood was ~50 μg/mL, thus showing low toxicity of PEG-GNRs.

The irradiated skin in the DSC model before and after injecting 0.44 mg of PEG-GNRs was harvested ~1 h after laser irradiation. The irradiated skin was prepared for a routine histological technique to examine the effect of PEG-GNRs on perivascular tissues during laser irradiation. In Fig. 12, no obvious side effects, such as coagulation of collagen, epidermal edema, and dermal damage, on the epidermis and dermis were observed before and after the injection of PEG-GNRs in mice when the targeted blood vessels were coagulated after laser irradiation. This result indicated that Nd:YAG laser irradiation combined with PEG-GNRs was a safe and effective method for the potential treatment of PWS.

Our study clearly showed that the evolution of targeted blood vessels after exposure to laser light and laser energy density and laser pulse required for photocoagulation and disappearance of blood vessels before and after injection of PEG-GNRs. However, directly observing the thermal response of PWS blood vessels in the clinic is difficult. In further clinical applications, the laser parameters and dosage of PEG-GNRs can be controlled by a noninvasive visualization system, such as the optical Doppler tomography (ODT)/optical coherence tomography (OCT) technique. Zhao et al.[30] first reported the clinical application of ODT to image and monitor blood flow in PWS birthmark before and after laser treatment. They also developed an imaging method utilizing velocity variance to determine the location and shape of blood vessels in human skin. Their findings provided a fast semiquantitative strategy

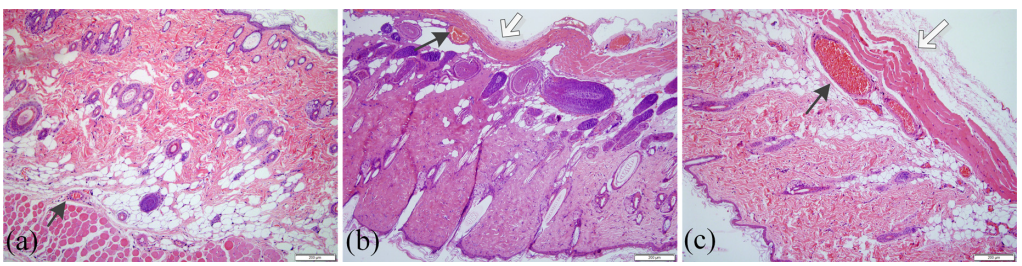

Fig. 12 (a) H&E-stained images of mice's skin preirradiation, (b) irradiated skin without PEG-GNRs exposed to Nd:YAG laser with energy density of 36 J/cm^2, and (c) irradiated skin with injection 0.44 mg of PEG-GNRs exposed to Nd:YAG laser with energy density of 31 J/cm^2 obtained at 1 h after laser irradiation. The white arrows indicate the direction of laser irradiation and the black arrows indicate the targeted blood vessels. The scale bars in all images are 200 μm.

to assess the clinical efficacy of PWS laser therapy. Similarly, Zhao et al.[31] developed a fiber OCT system to image PWS birthmark, which can be used to distinguish dilated PWS blood vessels from normal tissues. Moreover, epidermal thickness, diameter, and depth of dilated PWS blood vessels can be obtained. Photodynamic therapy (PDT) is another effective therapy for PWS. The consideration of PDT for the treatment of PWS is dependent on the epidermal thickness and the vascular distribution in human skin. In the past, surgeons selected the photosensitizer dose and laser parameters of PDT therapy for PWS mainly according to their clinical experience, leading to certain errors in adopting a similar treatment to different pathological types because the epidermal thickness and the vascular distribution vary from patient to patient. Using the OCT system, surgeons can formulate objective judgments of pathological types according to the thickness of the epidermis and the diameter and depth of dilated blood vessels, thereby treating PWS effectively with the optimal laser parameters and photosensitizer dosages.

In this study, we investigated the effect of PEG-GNRs on the thermal response of individual blood vessel using the mouse mesentery and DSC models, respectively. Although the ultrastructure of the postcapillary venules within the mice's skin is comparable to those in humans, mice's skin is thinner and contains some elements (e.g., subdermal muscle and numerous hair follicles) not seen in human skin. These differences between the mice's skin and PWS human skin may limit the clinical application of the preliminary data obtained from mouse models. Thus, more clinical trials should be conducted in the future to further examine the clinical effect of using PEG-GNRs as exogenous near-infrared laser absorbers to improve laser treatment of PWS.

4 Conclusion

Mouse mesentery and DSC models were used to analyze the thermal response of two vessel structures to Nd:YAG laser with and without PEG-GNRs. The mesentery results exhibited the thermal response of a single venule without other anatomic structures. This finding indicated that the threshold laser energy density required for blood coagulation and complete vasoconstriction decreased by 75%, 66%, 66%, and 64% after the injection of 0.44 mg of PEG-GNRs when laser energy density was 24, 27, 31, and 36 J/cm^2, respectively. The laser pulse required for complete vasoconstriction decreased by 75%, 66%, 60%, and 48%. The DSC model results showed the thermal response of subdermal blood vessels in the complex structure of skin. This finding indicated that the laser energy density required for blood coagulation and complete vasoconstriction decreased from 36 J/cm^2 without PEG-GNRs to 31 J/cm^2 after the injection of 0.44 mg of PEG-GNRs. After adding 0.44 mg of PEG-GNRs, the number of laser pulses required for blood coagulation decreased by 62.5%, 66.7%, 66.7%, and 74.3% when the laser energy was 24, 27, 31, and 36 J/cm^2, respectively. Similarly, the total number of laser pulses required for complete vasoconstriction decreased by 52.5%, 53.3%, 50.5%, and 61.5% when the laser energy was 24, 27, 31, and 36 J/cm^2, respectively. These results indicated that the Nd:YAG laser combined with PEG-GNRs can induce thermal damage to a single venule and blood vessels in the complex structure of skin with low laser energy density and minimal laser pulse.

The H&E stains of irradiated skin were obtained 1 h after laser irradiation, and the major organs were harvested 30 days after injecting 0.44 mg of PEG-GNRs. No epidermal and dermis damage in perivascular tissues were observed after laser irradiation combined with PEG-GNRs, and no toxicity of PEG-GNRs in the entire mouse life span occurred. Therefore, we assume that Nd:YAG laser irradiation combined with PEG-GNRs may be a promising approach to inducing irreversible damage to large blood vessels without adverse effects at low radiant exposure per pulse with minimal pulses.

Disclosures

No conflicts of interest.

Acknowledgments

The work was supported by the National Natural Science Foundation of China (grant number 51336006).

References

1. Z. F. Jasim and J. M. Handley, "Treatment of pulsed dye laser-resistant port wine stain birthmarks," *J. Am. Acad. Dermatol.* **57**(4), 677–682 (2007).
2. S. H. Barsky et al., "The nature and evolution of port wine stains: a computer-assisted study," *J. Invest. Dermatol.* **74**(3), 154–157 (1980).
3. G. Aguilar et al., "An overview of three promising mechanical, optical, and biochemical engineering approaches to improve selective photothermolysis of refractory port wine stains," *Ann. Biomed. Eng.* **40**(2), 486–506 (2012).
4. T. S. Alster and E. L. Tanzi, "Combined 595-nm and 1,064-nm laser irradiation of recalcitrant and hypertrophic port-wine stains in children and adults," *Dermatol. Surg.* **35**(6), 914–919 (2009).
5. R. Anderson and J. Parrish, "Selective photothermolysis: precise microsurgery by selective absorption of pulsed radiation," *Science* **220**(4596), 524–527 (1983).
6. D. Li et al., "Experimental study on the vascular thermal response to visible laser pulses," *Lasers Med. Sci.* **30**(1), 135–145 (2015).
7. D. Li et al., "A comparison of microvascular responses to visible and near-infrared lasers," *Lasers Surg. Med.* **46**(6), 479–487 (2014).
8. P. Yuan et al., "Plasmon coupling-enhanced two-photon photoluminescence of Au@Ag core-shell nanoparticles and applications in the nuclease assay," *Nanoscale* **7**(22), 10233–10239 (2015).
9. Z. Zhang et al., "Role of 5-aminolevulinic acid-conjugated gold nanoparticles for photodynamic therapy of cancer," *J. Biomed. Opt.* **20**(5), 051043 (2015).
10. P.-H. Wang et al., "Gold-nanorod contrast-enhanced photoacoustic micro-imaging of focused-ultrasound induced blood-brain-barrier opening in a rat model," *J. Biomed. Opt.* **17**(6), 061222 (2012).
11. Y.-C. Yeh, B. Creran, and V. M. Rotello, "Gold nanoparticles: preparation, properties, and applications in bionanotechnology," *Nanoscale* **4**(6), 1871–1880 (2012).
12. K. L. Kelly et al., "The optical properties of metal nanoparticles: the influence of size, shape, and dielectric environment," *J. Phys. Chem. B* **107**(3), 668–677 (2003).
13. B. Nikoobakht and M. A. El-Sayed, "Preparation and growth mechanism of gold nanorods (NRs) using seed-mediated growth method," *Chem. Mater.* **15**(10), 1957–1962 (2003).
14. X. H. Huang et al., "Plasmonic photothermal therapy (PPTT) using gold nanoparticles," *Lasers Med. Sci.* **23**(3), 217–228 (2008).
15. P. K. Jain et al., "Noble metals on the nanoscale: optical and photothermal properties and some applications in imaging, sensing, biology, and medicine," *Acc. Chem. Res.* **41**(12), 1578–1586 (2008).
16. L. Z. Xing et al., "Enhancement of light absorption by blood to Nd:YAG laser using PEG-modified gold nanorods," *Lasers Surg. Med.* **48**(8), 790–803 (2016).
17. L. Xing et al., "Nd:YAG laser-induced morphology change and photothermal conversion of gold nanorods with potential application in the treatment of port-wine stain," *Lasers Med. Sci.* **32**(3), 629–640 (2017).
18. X. C. Ye et al., "Using binary surfactant mixtures to simultaneously improve the dimensional tunability and monodispersity in the seeded growth of gold nanorods," *Nano Lett.* **13**(2), 765–771 (2013).

19. H. W. Liao and J. H. Hafner, "Gold nanorod bioconjugates," *Chem. Mater.* **17**(18), 4636–4641 (2005).
20. G. H. Algire, "An adaptation of the transparent chamber technique to the mouse," *J. Natl. Cancer Inst.* **4**, 1–11 (1943).
21. H. D. Papenfuss et al., "Transparent access chamber for the rat dorsal skin fold," *Microvasc. Res.* **18**(3), 311–318 (1979).
22. Z. F. Gourgouliatos et al., "Laser-irradiation-induced relaxation of blood vessels in vivo," *Lasers Surg. Med.* **10**(6), 524–532 (1990).
23. A. M. Geerts et al., "Increased angiogenesis and permeability in the mesenteric microvasculature of rats with cirrhosis and portal hypertension: an in vivo study," *Liver Int.* **26**(7), 889–898 (2006).
24. S. Zhang et al., "Ambient aqueous synthesis of ultrasmall PEGylated $Cu_{2-x}Se$ nanoparticles as a multifunctional theranostic agent for multimodal imaging guided photothermal therapy of cancer," *Adv. Mater.* **28**(40), 8927–8936 (2016).
25. B.-K. Wang et al., "Gold-nanorods-siRNA nanoplex for improved photothermal therapy by gene silencing," *Biomaterials* **78**, 27–39 (2016).
26. C. L. Didychuk et al., "Depth of photothermal conversion of gold nanorods embedded in a tissue-like phantom," *Nanotechnology* **20**(19), 195102 (2009).
27. E. J. Fiskerstrand et al., "Photothermally induced vessel-wall necrosis after pulsed dye laser treatment: lack of response in port-wine stains with small sized or deeply located vessels," *J. Invest. Dermatol.* **107**(5), 671–675 (1996).
28. X. Ren et al., "Surface modification and endothelialization of biomaterials as potential scaffolds for vascular tissue engineering applications," *Chem. Soc. Rev.* **44**(15), 5680–5742 (2015).
29. D. P. K. Lankveld et al., "Blood clearance and tissue distribution of PEGylated and non-PEGylated gold nanorods after intravenous administration in rats," *Nanomedicine* **6**(2), 339–349 (2011).
30. Y. H. Zhao et al., "Monitoring laser treatment of port wine stains using phase-resolved optical Doppler tomography," in *Coherence Domain Optical Methods in Biomedical Science and Clinical Applications IV*, pp. 237–242 (2000).
31. S. Zhao et al., "Imaging port wine stains by fiber optical coherence tomography," *J. Biomed. Opt.* **15**(3), 036020 (2010).

Bin Chen earned his PhD from Xi'an Jiaotong University, China, in 2002. He is currently a professor and vice director at the State Key Laboratory of Multiphase Flow in Power Engineering, Xi'an Jiaotong University. He has devoted his efforts to the research of photon propagation, heat transfer model, cryogen spray cooling, and biomedical application of nanomaterials related to laser dermatology. Currently, he serves as an editorial board member of *Journal of Clinical Dermatology and Therapy*.

Biographies for the other authors are not available.